Non-muffin-tin effects in the 4*d* transition metals Rb, Nb, and Pd†

G. S. Painter, J. S. Faulkner, and G. M. Stocks*
Metals and Ceramics Division, Oak Ridge National Laboratory, Oak Ridge, Tennessee 37830
(Received 31 October 1973)

While the effects of corrections to the muffin-tin model of the crystal potential have been investigated fairly thoroughly for various insulators and semiconductors, relatively few complete calculations have been done for transition metals. The Hartree-Fock-Slater muffin-tin approximate potential is usually adequate for characterization of the general properties of free-electron metals. In the transition-metals series, however, where the Fermi energy typically lies in a partially filled *d* band, it is recognized that small nonuniform energy shifts can appreciably alter the properties dependent upon the detailed topology of the Fermi surface. Here, we report the application of the recently proposed combined Korringa-Kohn-Rostoker discrete variational method for several crystals representative of the 4*d* transition-metal series. Results are analyzed directly in terms of the Bloch wave functions and various trends and general features of non-muffin-tin effects in the transition metals are determined.

INTRODUCTION

The Hartree-Fock-Slater (HFS) one-electron potential originating from the self-consistent-field model, upon which most energy-band calculations are based, is frequently approximated by a "muffin-tin" average. Within schemes using this model the Coulomb and local-density-dependent exchange-correlation potential[1] for an electron in the system is replaced by a spherical average within touching spheres and a constant in the interstitial region. This model has been of great value for obtaining a fairly reliable picture of the band structure of a large number of close-packed metallic systems, e.g., noble and transition metals. For simple metals a muffin-tin average of the HFS potential apparently produces no serious errors in the calculated eigenvalues, however it has been recognized for some time that for metallic systems with partially filled *d* bands the muffin-tin approximation can introduce small nonuniform shifts in the calculated energy bands. While these shifts are probably negligible in correlating band calculations with band-probe experiments such as photoemission, their effect upon details of the Fermi surface can be exaggerated when the Fermi energy lies in a region of flat bands. Inclusion of such shifts produce changes in the topology of the Fermi surface which are well within the observable range of experiments such as those based upon the de Haas-van Alphen effect.

In order to study the effects of potential anisotropy it is necessary to have available a very precise energy-band method which is capable both of treating non-muffin-tin potentials, and of accurately calculating the resulting small eigenvalue shifts. Here we report a systematic application of the recently proposed Korringa-Kohn-Rostoker discrete variational method[2] (KKR-DVM) to the calculation of non-muffin-tin shifts in a series of 4*d* transition metals. The KKR-DVM scheme was not specifically developed for treating metallic systems but rather for treating compounds, molecular complexes, and atomic clusters, where the limitations of the muffin-tin model are more serious. However, its computational accuracy and numerical efficiency make it an ideal method for efficiently obtaining a comprehensive survey of the non-muffin-tin effects in the transition metals.

We have chosen as illustrative cases Rb, Nb, and Pd from the 4*d* transition-metal series, these presumably being representative of the full 4*d* series. Rb, traditionally regarded as a free-electron-like system, has an unoccupied *d*-band complex just above the Fermi energy; thus in certain respects it may be viewed as a transition metal with unoccupied *d* bands. The *d* bands in Nb bracket the Fermi energy; in the atom Nb has a $4d^4 5s^1$ configuration, thus in the solid the *d*-band complex is approximately half filled, the Fermi energy lying just below the *s*-*d* hybridization gap typical of bcc transition metals and intersecting a rather flat band near the zone center. In Pd the *d* bands are almost filled, the Fermi energy falling in a region where there are very flat bands and hence a high density of states, a situation where it might be expected that non-muffin-tin effects would be of some consequence. The calculations show the non-muffin-tin corrections to be important in Nb, but of little significance in Pd; the reasons for this behavior require an analysis of the relevant eigenstates.

While there have been a number of attempts to remove the muffin-tin restrictions in the past (see Painter[2] and references therein) the present calculation represents the first application to a transition-metal series of a general band-structure method which is capable of giving definitive estimates of the small energy shifts involved and thus facilitates a discussion of the characteristic trends in a given transition metal series, and will therefore serve to clarify the importance of non-muffin-tin

effects in transition metals in general.

In Sec. II we briefly review the salient features of the KKR-DVM approach and in Sec. III we present the results of the calculations for Rb, Nb, and Pd. Section IV comprises some general conclusions and some comments on the adequacy of the muffin-tin-model for the transition metals.

II. METHOD

An accurate treatment of the rather small non-muffin-tin perturbations in the transition metals necessitates a technique which is flexible enough to calculate the interactions over the entire unit cell with sufficiently high precision. The combined KKR-DVM approach, although devised mainly for crystal compounds, provides an easily implemented procedure to treat these problems for the transition metals. The description of the method here will be brief, as a more detailed account already appears in the literature.[2]

The basic problem is to find approximate solutions to the eigenvalue problem

$$H(\vec{r})\,\psi_i(\vec{k},\vec{r}) = [-\nabla^2 + V(\vec{r})]\,\psi_i(\vec{k},\vec{r}) = E_i(\vec{k})\,\psi_i(\vec{k},\vec{r}), \tag{1}$$

where $V(\vec{r})$ is a general non-muffin-tin potential. We seek eigenfunctions expressible in terms of some fixed Bloch basis

$$\psi_i(\vec{k},\vec{r}) = \sum_j \chi_j(\vec{k},\vec{r})\,C_{ji}(\vec{k}). \tag{2}$$

In the KKR-DVM approach the trial basis set is constructed directly from the KKR solutions to the muffin-tin average of the full Hamiltonian. These can be written[3]

$$\chi_i(\vec{k},\vec{r}) = \sum_{l,m} i^l\,C_{lm}(\vec{k})\,Y_{lm}(\Omega) \times \begin{cases} u_l(r), & r \le R_0 \\ N_l[j_l(\alpha r) - \tan\eta_l n_l(\alpha r)], & r > R_0 \end{cases} \tag{3}$$

where η_l is the phase shift, $\alpha = \sqrt{E}$, R_0 is the sphere radius and

$$N_l = \alpha R_0^2 \left(u_l \frac{dn_l}{dr} - \frac{du_l}{dr} n_l\right)_{r=R_0}.$$

The coefficients C_{lm} are determined upon solving for the KKR muffin-tin eigenvalues.

Partitioning the full Hamiltonian $H(\vec{r})$ into a usual muffin-tin form $H_0(\vec{r})$ with a muffin-tin average potential $V_0(\vec{r})$, and the non-muffin-tin corrections $\Delta V(\vec{r})$, we have

$$H(\vec{r}) = H_0(\vec{r}) + \Delta V(\vec{r}). \tag{4}$$

Solutions to the muffin-tin Hamiltonian are obtained using the KKR method[4]

$$H_0(\vec{r})\,\chi_i(\vec{k},\vec{r}) = [-\nabla^2 + V_0(\vec{r})]\,\chi_i(\vec{k},\vec{r}) = \epsilon_i(\vec{k})\,\chi_i(\vec{k},\vec{r}) \tag{5}$$

and used to calculate the necessary perturbative corrections to the secular equations, i.e.,

$$\langle\chi_i|H(\vec{r})|\chi_j\rangle = \langle\chi_i|\epsilon_j + \Delta V(\vec{r})|\chi_j\rangle = \epsilon_j\delta_{ij} + \langle\chi_i|\Delta V(\vec{r})|\chi_j\rangle. \tag{6}$$

In the metals considered here, the non-muffin-tin terms do not significantly couple different band states of like symmetry, hence the corrections are simply first-order shifts of the levels. The numerical-integration procedures used to calculate the perturbation matrix elements are essentially the same as those described in previous applications.[5] The corrections are evaluated by integrals over a single unit cell of the crystal, here treated by point sampling with some preselected point density $w^{-1}(\vec{r})$, i.e.,

$$\langle\chi_i|\Delta V(\vec{r})|\chi_j\rangle \simeq \sum_{m=1}^{M} w(\vec{r}_m)\chi_i^*(\vec{k},\vec{r}_m)\,\Delta V(\vec{r}_m)\,\chi_j(\vec{k},\vec{r}_m). \tag{7}$$

With no significant coupling among the KKR eigenfunctions through the non-muffin-tin perturbation $\Delta V(r)$, the calculation reduces to the diagonal elements of the perturbation matrix.

III. RESULTS

A. General discussion

We have calculated the shifts in the eigenvalues which result from non-muffin-tin effects in Rb, Nb, and Pd at certain high-symmetry points and along certain symmetry directions for the occupied part of the conduction band complex and for a few energies above the filled region, sufficient to include the d-band structure in the unoccupied bands of Rb. Table I shows a compilation of energy shifts at the Brillouin zone center for Rb, Nb, and Pd as well as the change in the d band width and s-d band separation which results from the inclusion of non-muffin-tin effects. The shifts are given in terms

TABLE I. Important non-muffin-tin shifts in Rb, Nb, Pd, and Ni.

	$\delta E = E^{\text{KKR-DVM}} - E^{\text{KKR}}$ (Ry)			
Level	Rb	Nb	Pd	Ni
Γ_1	0.000	−0.002	0.001	+0.003
$\Gamma_{25'}$	−0.003	−0.010	−0.003	0.000
$\Gamma_{12'}$	0.000	0.008	−0.000	−0.002
X_1			0.010	0.010
X_3			−0.004	−0.003
X_2			−0.002	0.001
X_5			0.000	−0.001
$X_{4'}$			−0.012	−0.009
H_{12}	0.003	0.010		
$H_{25'}$	0.000	−0.002		
s-d separation[a]	0.003	0.012	0.009	0.013
d width[b]	−0.003	−0.011	−0.010	−0.011

[a]For bcc H_{12}-Γ_1; for fcc X_1-Γ_1.
[b]For bcc $H_{25'}$-H_{12}; for fcc X_5-X_1.

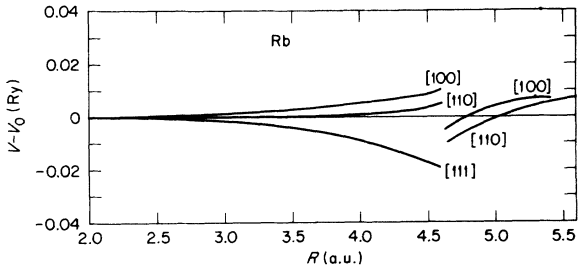

FIG. 1. Non-muffin-tin potential corrections $\Delta V = V - V_0$ along crystallographic directions in Rb; V represents the full crystal HFS potential and V_0 its muffin-tin average.

of $\delta E = E^{\text{KKR-DVM}} - E^{\text{KKR}}$; also included in the table for comparison is similar data for the 3*d* transition metal Ni, which has previously been discussed by Painter.[2] Perhaps the most significant point to note in the table of shifts is that in terms of the resolution of most band probe experiments the shifts are small. Energy shifts associated with the low-lying *s*-like levels in all three systems are always small (<0.005 Ry). There is a clear trend for the 4*d* systems in *d*-like level shifts, the shifts being

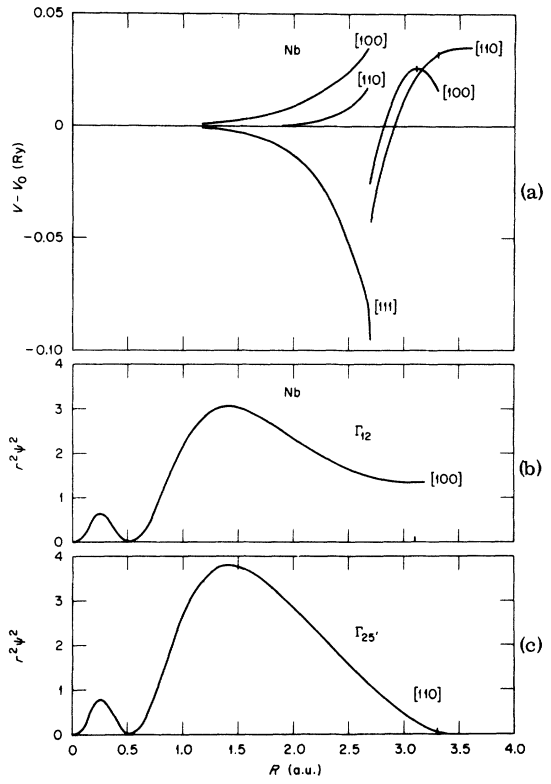

FIG. 2. (a) Potential perturbations, and (b) and (c) radial charge densities of *d*-band states at Γ in Nb.

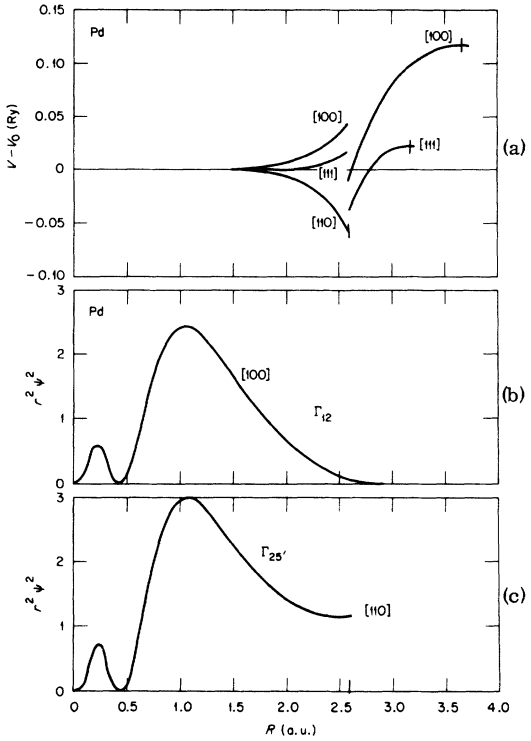

FIG. 3. (a) Non-muffin-tin potential corrections and (b) and (c) radial densities of zone-center *d* states for Pd.

nearly zero in Rb, about 0.01 Ry in Nb, and again small in Pd—about 0.005 Ry. The increase in *s-d* band separation and the narrowing of the *d*-band complex which results from the lifting of the lower *d*-like states and lowering of the upper *d*-like states is a feature common to Nb and Pd (and also Ni) and thus seems to represent a feature of the inclusion of non-muffin-tin effects which is independent of the crystal structure of the system.

In order to gain a complete understanding of the origin of the observed shifts and the over-all trends, it is necessary to consider the details of the respective crystal wave functions as well as the behavior of the non-muffin-tin potential corrections ΔV along various crystallographic directions in the unit cell of the crystal. Examination of plots of the radial charge densities for the *d*-symmetry levels and non-muffin-tin corrections appearing in Figs. 1–3 makes it clear that rather complicated effects of the angular and radial dependencies of the orbitals, coupled with those of the potential, are operative.

For bcc Rb the free atom potential is nearly constant at the crystalline internuclear separation of 10.74 a.u. thus, as illustrated in Fig. 1 the deviations of the crystal potential about an atom site from that of sphericity are quite small (less than 0.02 Ry). The eigenfunctions (not illustrated) are

nearly constant in the volume outside the muffin-tin spheres and negligible shift originates in that region. Although corrections from inside the sphere are somewhat larger and the radial dependence of the states more pronounced, these lead to only a small shift (−0.003 Ry) of the $\Gamma_{25'}$ level. As will be discussed below, this primarily results from the negative potential correction along the [111] direction. Since the Fermi energy lies in an s band, the level shifts leave the Fermi-surface characteristics essentially unchanged.

For Nb, as we see from Fig. 2(a), the non-muffin-tin potential corrections are large not only in the interstitial volume but also inside the muffin-tin spheres. Particularly noteworthy is the large negative potential correction inside the spheres originating from the near-neighbor Nb atomic overlaps along directions equivalent to the [111]. For illustrative purposes we will consider the d_{xy} member of the triply degenerate set of $\Gamma_{25'}$ eigenfunctions (d_{xy}, d_{xz}, d_{yz}) and the $d_{x^2-y^2}$ member of the Γ_{12} doublet throughout this discussion. The radial charge densities calculated from these states appear in Fig. 2(b) and 2(c), respectively. The single most important feature of the non-muffin-tin effects for Nb is the interaction of the $\Gamma_{25'}$ state with the "inside" potential corrections in the [111] directions. Although the lobes of the $\Gamma_{25'}$ states point in directions typified by the [110], the shifts resulting from the inside and outside corrections from these regions are very nearly cancelling. While the "outside" correction becomes rather large and positive in the [110] directions the orbital density becomes vanishingly small at the unit cell edges where ΔV is largest. Furthermore in the [110] directions the negative shift coming from the volume immediately outside the muffin tins is approximately cancelled by the positive shift originating from the corrections inside the muffin-tin spheres. In these regions the radial density is monotonically decreasing with increasing r. The greatest part of the shift of the $\Gamma_{25'}$ level originates from the overlap of the orbitals inside the muffin-tin spheres with the large negative ΔV contribution along the near-neighbor [111] directions. The negative enhancement originating from the [111] directions is much smaller for the Γ_{12} states which have lobes that point along [100] directions and thus "avoid" the near-neighbor sites.

The origin of the shift of the Γ_{12} level is clearly the direct effect of the large positive corrections along the [100] directions again originating predominantly inside the muffin-tin sphere. The potential correction along [100] changes sign outside the muffin-tin sphere, with some resulting cancellation effects since the Γ_{12} radial density is essentially constant in these directions. The interaction of Γ_{12} states with the potential corrections along [110] directions is small with a near cancellation between the inside and outside parts. It is clear from the origin of the non-muffin-tin shifts in Nb that a warped muffin-tin treatment would be quite inadequate and this is substantiated from the results of Table II. As will be discussed subsequently these shifts appreciably affect the details of the Fermi surfaces since E_F lies in the d bands with an intersection of bands lying very close to the $\Gamma_{25'}$ state.

Comparing the difference potential plots of Nb and Pd in Figs. 2(a) and 3(a) (noting the difference in scales) it is interesting to observe that the corrections ΔV are generally larger for Pd than Nb. However, from the results of Table III, it is clear that eigenvalue shifts of the d levels are not nearly as sensitive to the potential corrections in Pd as in Nb. Part of this behavior relates to the fact that the maximum in the radial density is contracted by about 30% in Pd over that in Nb. From Fig. 3(b) it is quite apparent that the Γ_{12} level is affected little by the non-muffin-tin corrections since the radial density is very small in the interstitial volume and the inside corrections are nearly self-can-

TABLE II. Non-muffin-tin shifts in niobium (Ry units). Muffin-tin levels are denoted E_0, shifts therefrom with full potential δE, and shifts in warped muffin-tin approximation δE_{WMT}.

Level	E_0	δE	δE_{WMT}	Ratio
Γ_1	−1.0076	−0.0016	0.0000	0.00
Γ_{12}	−0.4400	+0.0076	+0.0016	0.21
$\Gamma_{25'}$	−0.6196	−0.0098	−0.0038	0.39
H_{12}	−0.9172	+0.0094	+0.0032	0.34
$H_{25'}$	−0.2720	−0.0018	−0.0006	0.33
δ (d-bandwidth)		−0.0112	−0.0038	0.34

TABLE III. Comparison of warped muffin-tin and full non-muffin-tin shifts in the lowest conduction band eigenvalues in Pd. The warped muffin-tin shifts are those presented in Table IX of Ref. 6. Energies are in Ry.

Nonrelativistic level	Relativistic level	Warped muffin-tin shift	KKR-DVM shift
Γ_1	Γ_{6^+}	−0.0007	0.0001
$\Gamma_{25'}$	Γ_{8^+}	−0.0024	−0.0026
	Γ_{7^+}	−0.0025	
Γ_{12}	Γ_{8^+}	−0.0010	0.0000
X_1	X_{6^+}	0.0047	0.0096
X_3	X_{7^+}	−0.0047	−0.0046
X_2	X_{7^+}	−0.0002	0.0010
X_5	X_{6^+}	−0.0002	−0.0004
	X_{7^+}	−0.0002	
$X_{4'}$	X_{6^-}	−0.0112	−0.0122
L_1	L_{6^+}	−0.0054	−0.0056
L_3	L_{4^+}	−0.0015	−0.0004
	L_{6^+}	−0.0015	
L_3	L_{7^+}	−0.0002	+0.0004
	L_{6^+}		

celling. Similarly although the $\Gamma_{25'}$ level interaction with the negative difference potential along the [110] directions is large, it is diminished by the positive contribution from the other principal directions. The shift is quite small however, and apparently since the KKR-DVM and warped muffin-tin shifts are nearly the same for this level, the contributions of the [111] directions outside the muffin-tins represent the dominant effect.

Although the zone center states in Pd are little affected by the non-muffin-tin perturbations, the situation is quite different for levels at the symmetry point X. The presence of angular terms with $l>2$ in the wavefunctions complicates the analysis somewhat but the following general observations can be made. With the exception of the X_1 level, the non-muffin-tin shifts are within about a millirydberg of those calculated by Koelling *et al.*[6] using the warped muffin-tin approximation of ignoring the non-muffin-tin perturbations inside the spheres. The d-like level X_5, which is important in determining the details of the Fermi surface of Pd, shifts by less than 1 mRy. The radial density for this level plotted in the [111] direction is nearly the same as that for the Γ_{12} state in the [100] direction [Fig. 3(b)], and results in the relative insensitivity of this level to the non-muffin-tin perturbations. Thus of the cases studied here, only the non-muffin-tin corrections for Nb appear to possibly significantly affect the Fermi-surface topology and in Sec. III D we will examine this in more detail.

B. Calculated bands

The KKR calculations which were carried out for the muffin-tin potentials in order to generate variational basis sets for input to the KKR-DVM program, utilized a symmetrized version[7] of earlier KKR programs.[8] As we have already indicated in Rb the shifts in the energy bands introduced by including the non-muffin-tin effects are essentially zero, therefore the energy band structure is unaltered from the muffin-tin results. Although there are fairly substantial (0.005–0.010 Ry) energy shifts in certain energy levels in Pd, the shifts occur mainly in levels which are far below the Fermi energy, e.g., X_1, L_1, X_3. For the remaining levels the energy shifts are usually less than 0.002 Ry (see Table III, for example) except for the $X_{4'}$ level lying approximately 0.3 Ry above E_F which experiences a shift of -0.012 Ry. Thus, the non-muffin-tin shifts in Pd appear to be well accounted for by the warped muffin-tin model of Koelling *et al.*[6] For all practical purposes, the non-muffin-tin band structure of Pd may be taken as that given by the augmented-plane-wave (APW) muffin-tin calculation of Mueller *et al.*[9]

In the case of Nb the energy level shifts are

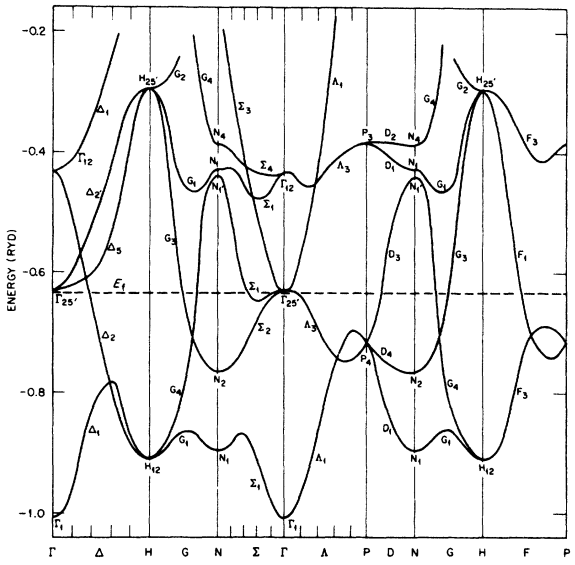

FIG. 4. KKR-DVM band structure of niobium.

larger than in Pd by generally a factor of 2. Figure 4 shows the band structure of Nb obtained using the combined KKR-DVM scheme with non-muffin-tin effects included. E_F gives an estimate of the Fermi energy (see Sec. III C). The corrections were explicitly calculated at the symmetry points Γ, H, N, and P and along the directions Δ, Σ, and Λ; the bands along the directions G, D, and F were drawn in using the end point data and some earlier band structures[10,11] and are included as a guide to the eye. The most significant changes in the band structure of Fig. 4 from the corresponding muffin-tin calculation are along the Σ direction, and in Fig. 5 we plot the Σ direction bands which are in the neighborhood of the Fermi surface and which are therefore important in determining many of the Fermi-surface features. The dashed curve in Fig. 5 shows the Σ_1 and Σ_2 bands obtained using the muffin-tin potential, the solid line gives the corresponding bands for the full non-muffin-tin potential. The label E_F^{KKR} marks the Fermi energy for the muffin-tin potential as calculated using the techniques described by Faulkner *et al.*[8] This energy is accurate to approximately 0.001 Ry for the potential function used. The estimated Fermi energy for the non-muffin-tin bands is designated by $E_F^{\mathrm{KKR\text{-}DVM}}$. In Fig. 6 we further analyze the Σ_1 and Σ_2 bands in terms of the energy shifts $\delta E = E^{\mathrm{KKR\text{-}DVM}} - E^{\mathrm{KKR}}$ between the non-muffin-tin and muffin-tin band structures. The large uniform shift in the Σ_2 band is the largest such effect observed upon including the non-muffin-tin corrections although from the point of view of affecting measured properties which depend on the Fermi surface the nonuniform shifts in the Σ_1 band which result in a flattening of the

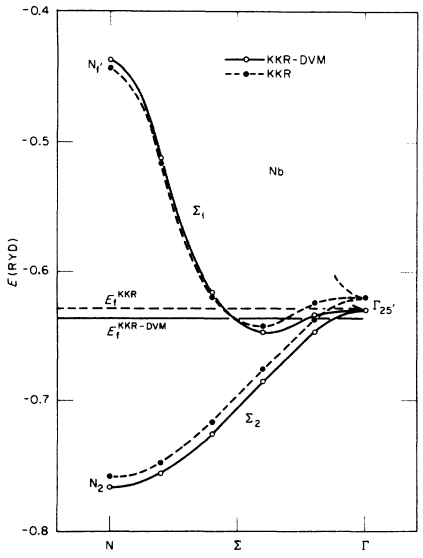

FIG. 5. Non-muffin-tin shifts of the energy bands of Nb along the Σ direction; dashed curve represents KKR muffin-tin bands, the solid curve denotes KKR-DVM results with full potential.

band are of more significance, since this band intersects the Fermi surface twice and hence is of great importance in determining the fine details of the Fermi surface. These effects result mostly from the downward shift of the $\Gamma_{25'}$ level, a result which can be understood in terms of the spatial variation of the KKR wave function. From this point of view it seems that the details of the Nb Fermi surface are particularly sensitive to fairly small non-muffin-tin effects because of the close proximity of the $\Gamma_{25'}$ level to the Fermi energy. The magnitude of the density of states at the Fermi energy is similarly sensitive and presumably increased over the muffin-tin value because of the flattening of the Σ_1 band. We will return to a discussion of the modification expected in the Fermi-surface dimensions of Nb later in this section.

C. Comparison with warped muffin-tin calculations

Koelling *et al.*[5] have discussed the effect of including non-muffin-tin corrections into the band structure of Pd. In their warped muffin-tin relativistic APW calculation the effects of deviations from the constant potential outside the muffin-tin sphere are included. Inclusion of warped-muffin-tin effects in the band calculation produces shifts generally of the order of 0.002 Ry except for the lowest-lying levels at the X point, L point, and W point which are of the order of 0.005 Ry and for the level X_6 which is shifted by -0.011 Ry. Since the calculation of Koelling *et al.* included relativistic effects we cannot make a rigorous comparison with their results, however in Table III we associate the nonrelativistic level with its corresponding relativistic level and compare the warped muffin-tin shifts with the shifts obtained in this work, which include not only the warped muffin-tin effects but also deviations of the full potential from spherical symmetry inside the muffin-tin spheres. From the table it is clear that the largest fraction of the non-muffin-tin corrections to the eigenvalues in Pd is a consequence of deviations of the crystal potential from a constant in the interstitial region, thus for Pd at least the warped muffin-tin model appears to be adequate. This is not the case for Nb.

In Table II we have made a comparison of the warped muffin-tin shifts with the full non-muffin-tin shifts for a few eigenvalues at Γ and H for Nb. For Nb we calculated the warped muffin-tin corrections using the combined KKR-DVM scheme by setting the potential perturbation equal to zero inside the spheres. As can be seen from the table, warped muffin-tin effects generally only account for about 35% of the total energy shift. Thus, for Nb the warped muffin-tin approximation would be inadequate for discussing the effects of crystal potential deviations from the muffin-tin form. This contrasting behavior of Nb and Pd can again be simply understood in terms of the spatial extent of the d-like function associated with the atomic sites, these being more diffuse in Nb than in Pd, hence tails from neighboring sites overlap more in Nb than in Pd. Thus, as a general statement it should be expected that the warped-muffin model would be adequate at each end of a transition-metal series but would be increasing less adequate towards the center of the series.

D. Fermi-surface effects

In the case of Rb, inclusion of non-muffin-tin effects would have essentially no effect on the Fermi-surface properties of the metal. In the case of Pd, although the shifts in energy levels in the neighbor-

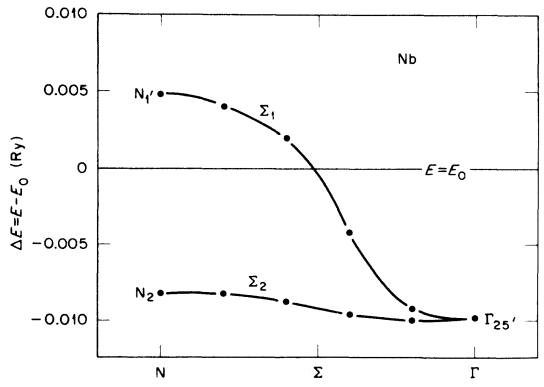

FIG. 6. Band shifts in Nb along the Σ direction.

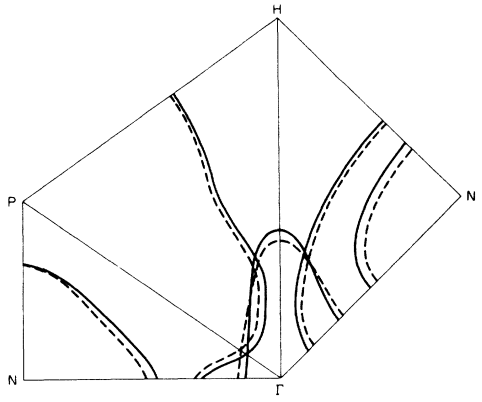

FIG. 7. Intersections of the Nb Fermi surface with central {100} and {110} planes; dashed lines denote KKR results, the solid lines represent the estimated Fermi surface upon including non-muffin-tin shifts.

hood of the Fermi surface are small, except for the level X_4', these shifts can have sizable effects on Fermi-surface dimensions as was pointed out by Koelling *et al.*[6] However, since the warped muffin-tin approximation gives most of the effect for the states in the neighborhood of the Fermi energy, the remarks made by Koelling *et al.* on these Fermi-surface changes carry over to the present calculation.

For Nb, the Fermi surface, which we have obtained in the KKR calculation is topologically equivalent to that obtained by Mattheiss[10] using the APW method. While we have not calculated Fermi-surface extremal areas it appears that the present muffin-tin band calculation would give orbits essentially identical to those obtained by Mattheiss. While it is impossible to calculate in any quantitative fashion the changes in the Nb Fermi surface when non-muffin-tin corrections have been included in the Nb potential using only the few eigenvalues which we have calculated, it is possible to make some qualitative statements. In order to estimate the Fermi energy we have taken the point of view that E_F is essentially tied to changes in the position of the $\Gamma_{25'}$ eigenvalue and the rather flat band Σ_1 (see Fig. 5) in the neighborhood of Γ. Accordingly, we have taken E_F to be in the same position relative to $\Gamma_{25'}$ and the Σ_1 band minimum in the KKR-DVM calculation as in the KKR calculation, this fixes E_F at -0.636 Ry. From this and the band structure of Fig. 4 it is possible to obtain qualitative changes in Fermi-surface dimensions along symmetry directions. The result of this analysis is shown in Fig. 7. The dotted lines show the Fermi surface for the $\Sigma\Lambda$, $\Lambda\Lambda$, $\Sigma\Delta$ planes obtained using the KKR constant-energy search procedures outlined by Faulkner *et al.*[8]; the solid line shows the Fermi surface estimated from the KKR-DVM results. It should be stressed that the solid line is fixed at only a few points along symmetry directions and thus the solid curve should be regarded as little more than a guide to the eye. From this picture it is clear that the size of the Γ-centered "jungle gym" is decreased while the N-centered "ellipsoids"[10] are increased in size by the inclusion of non-muffin-tin effects. Although the jungle-gym structure is generally decreased in size it appears doubtful upon studying Fig. 7 that the minimum arm radius of the jungle gym in Nb is decreased by inclusion of the non-muffin-tin effects. Mattheiss[10] concluded on the basis of Hall data[12] that his muffin-tin calculation underestimated this extremum; we would conclude that inclusion of non-muffin-tin effects would not help improve agreement with experiment. The largest discrepancy of the muffin-tin results with magnetothermal oscillation[13] and de Haas–van Alphen data,[13,14] i.e., the minimum area on the jungle gym, would not be resolved by the non-muffin-tin shifts.

Turning to the ellipsoids at N, based on the results of Mattheiss, the muffin-tin-potential calculation compared with experiment appears to overestimate the extremal areas of the ellipsoids. Since non-muffin-tin corrections serve to enlarge these structures by as much as 12% of the radius vector of the surface along the G direction again we must conclude that inclusion does not help bring the calculated areas into better agreement with experiment.

That inclusion of non-muffin-tin effects does not help bring the calculated Fermi surface of Nb into agreement with experiment should not be too surprising since an inspection of atomic data (e.g., Herman and Skillman[15]) suggests that systematic inclusion of mass-velocity, Darwin, and spin-orbit terms in the Hamiltonian would introduce shifts in the eigenvalues of the same order as those introduced by the inclusion of non-muffin-tin effects. In the atom inclusion of mass-velocity and Darwin terms increases the s-d atomic level separation by approximately 0.011 Ry, while spin-orbit coupling introduces a splitting of approximately 0.016 Ry in the $d_{3/2}$, $d_{5/2}$ levels. Similar effects would be expected in the solid, an increase in the separation of the d bands with respect to the s-p band and removal of certain degeneracies in the d band. In particular the $\Gamma_{25'}$ level which is important in determining details of the Fermi surface would be split by inclusion of spin-orbit coupling into a Γ_{7+} and a Γ_{8+} state, by an amount of the same order of magnitude as the shift in the $\Gamma_{25'}$ level introduced by the inclusion of non-muffin-tin terms.

From the foregoing it is clear that in order to obtain a detailed picture of the Fermi surface of Nb a calculation which includes the influence both of non-muffin-tin corrections and of relativistic ef-

fects will have to be made, since the details of the Fermi surface are obviously sensitive to such minor shifts.

IV. CONCLUSIONS

From the results of these calculations it appears that systematic inclusion of non-muffin-tin effects in the crystal potentials for 4d transition metals produces only minor modifications (less than 0.02 Ry) to the energy band structure obtained using the muffin-tin approximation. That is not to say that they are insignificant, particularly for Nb and to a lesser extent Pd, and presumably for metals near the center of each transition metal series, since they can produce changes in Fermi-surface dimensions which could clearly be observed in present-day high-precision de Haas–van Alphen experiments. However, on the scale of the resolution of most band probe experiments and indeed of our understanding of the magnitude of exchange and correlation effects, the shifts are quite small. Thus contrary to some recent speculation[16] it appears that not only does the muffin-tin approximation allow for a physically appealing understanding of the general properties of transition metals through the d-scattering resonance picture, but also if the scheme is implemented fully it will produce reliable band parameters.

As might have been anticipated, for the sequence Rb, Nb, and Pd the corrections to the band structure due to non-muffin-tin effects are greatest in Nb. Analysis of the crystal eigenfunctions has shown that this is related to both the spatial extent and angular variation of the eigenfunction and potential perturbation. In Rb the potential perturbation is everywhere small hence all eigenvalue shifts are essentially zero. In Nb the potential perturbation is quite large, both inside and outside of the muffin-tin sphere volume, most significantly, along the near neighbor bonding directions. For s-like states the angular variation is averaged to produce a near zero energy shift, however for d-like states this is generally not the case with the result that there are shifts of about 0.01 Ry in the zone center eigenvalues Γ_{12} and Γ_{25}. A detailed spatial analysis of the wave function and potential makes it clear that these shifts in Nb are due primarily to deviations of the potential function from the muffin-tin form inside the muffin-tin sphere, warped muffin-tin effects only accounting for a secondary part of the shifts. In this respect Pd contrasts sharply with Nb where the correction to the d-like levels appear to originate primarily from deviations of the full potential from the muffin-tin form in the interstitial volume, and hence are well accounted for by the warped muffin-tin model. Although the non-muffin-tin potential perturbations are as large in Pd as those in Nb, the differences in crystallographic bonding accounts for an effective cancellation of perturbative effects originating inside the muffin-tin spheres.

In Nb the main results of the changes introduced in the topology of the Fermi surface by non-muffin-tin corrections are to increase the size of the N-centered hole ellipsoids and to correspondingly decrease the size of the Γ-centered jungle-gym hole surface. It appears that both of these effects only serve to make worse the rather good agreement for Fermi-surface dimensions obtained between a non-self-consistent nonrelativistic muffin-tin calculation and experiment. Herein seems to be the problem in fully testing the Hartree-Fock-Slater model for crystals in terms of Fermi-surface dimensions in these systems. The Fermi surface is relatively sensitive to rather minor shifts in the bands near the Fermi energy, thus until a calculation is performed which includes all of the above effects, self-consistency, relativistic, and non-muffin-tin, it is impossible to make definitive statements about the Fermi-surface details. In particular, the inclusion of relativistic effects can produce shifts of the same order as those introduced by the inclusion of non-muffin-tin effects. In the case of Nb, it can be estimated from atomic calculations that the mass-velocity and Darwin corrections lead to a 5s-4d level separation change of about 0.01 Ry. The spin-orbit effects which are so crucial to the Fermi-surface topology are also sizable, for the 4d levels amounting to approximately 0.015 Ry.

Finally, mention should be made of the computational efficiency of the combined KKR-DVM scheme which we have used to perform these calculations. For the transition metals treated in this work, well converged KKR wave functions which are the input basis set for the DVM are readily obtained from standard symmetrized KKR programs with angular maximum sums of $l=4$. The resultant small basis set of symmetrized KKR orbitals reduces the calculation of the non-muffin-tin corrections to the KKR eigenvalues to a rather trivial matter compared with the effort which would be required for standard linear-combination-of-atomic-orbitals (LCAO) type procedures. From the point of view of future work with the KKR-DVM scheme in systems where non-muffin-tin effects have more serious consequences, provided suitably converged KKR wave functions can be obtained, calculation of the energy shifts due to non-muffin-tin effects should go through with little more effort than was required for the present calculation.

ACKNOWLEDGMENT

One of us (G. M. S.) would like to acknowledge the kind hospitality of the Metals and Ceramics Division of Oak Ridge National Laboratory during a short summer visit in which period this paper was written.

†Research sponsored by the U.S. Atomic Energy Commission under contract with the Union Carbide Corp.

*Present address: H. H. Wills Physics Laboratory, University of Bristol, Bristol, United Kingdom.

[1]J. C. Slater, Phys. Rev. 81, 385 (1951).

[2]G. S. Painter, Phys. Rev. B 7, 3520 (1973).

[3]P. M. Morse, Proc. Natl. Acad. Sci. U.S. 42, 276 (1956); A. R. Williams, S. M. Hu, and D. W. Jepsen,
[4] in *Computational Methods in Band Theory*, edited by P. M. Marcus, J. F. Janak, and A. R. Williams (Plenum, New York, 1971), p. 157.

[4]J. Korringa, Physica (Utr.) 13, 392 (1947); W. Kohn and N. Rostoker, Phys. Rev. 94, 1111 (1954).

[5]D. E. Ellis and G. S. Painter, Phys. Rev. B 2, 2887 (1970).

[6]D. D. Koelling, A. J. Freeman, and F. M. Mueller, Phys. Rev. B 1, 1318 (1970).

[7]J. S. Faulkner, Bull. Am. Phys. Soc. 16, 313 (1971).

[8]J. S. Faulkner, H. L. Davis, and H. W. Joy, Phys. Rev. 161, 656 (1967).

[9]F. M. Mueller, A. J. Freeman, J. O. Dimmock, and A. M. Furdyna, Phys. Rev. B 1, 4617 (1970).

[10]L. F. Mattheiss, Phys. Rev. B 1, 373 (1970).

[11]J. R. Anderson, D. A. Papaconstantopoulos, J. W. McCaffrey, and J. E. Schirber, Phys. Rev. B 7, 5115 (1973). As noted by these authors, their self-consistent APW results are in over-all quantitative agreement with those of Mattheiss (Ref. 10). Our analysis of these results is then expected to be valid within a self-consistent framework also.

[12]E. Fawcett, W. A. Reed, and R. R. Soden, Phys. Rev. 159, 533 (1967); W. A. Reed and R. R. Soden, Phys. Rev. 173, 677 (1968).

[13]M. H. Halloran, J. H. Condon, J. E. Graebner, J. E. Kunzler, and F. S. L. Hsu, Phys. Rev. B 1, 366 (1970).

[14]G. B. Scott and M. Springford, Proc. R. Soc. A 320, 115 (1970).

[15]F. Herman and S. Skillman, *Atomic Structure Calculations* (Prentice-Hall, Englewood Cliffs, N.J., 1963).

[16]J. Friedel, J. Phys. F 3, 785 (1973).